Available online at www.sciencedirect.com
SCIENCE DIRECT®
Journal of Magnetic Resonance 171 (2004) 225–232
JMR Journal of Magnetic Resonance
www.elsevier.com/locate/jmr

An NMR study of the origin of dioxygen-induced spin-lattice relaxation enhancement and chemical shift perturbation

R. Scott Prosser[a,*], Paul A. Luchette[b]

[a] Department of Chemistry, University of Toronto, UTM, 3359 Mississauga Rd. North, Mississauga, Ont., Canada L5L 1C6
[b] Department of Chemistry, Kent State University, USA

Received 21 April 2004; revised 18 August 2004
Available online 25 September 2004

Abstract

Due to its depth-dependent solubility, oxygen exerts paramagnetic effects which become progressively greater toward the hydrophobic interior of micelles, and lipid bilayer membranes. This paramagnetic gradient, which is manifested as contact shift perturbations (^{19}F and ^{13}C NMR) and spin-lattice relaxation enhancement (^{19}F and ^{1}H NMR), has been shown to be useful for precisely determining immersion depth, membrane protein secondary structure, and overall topology of membrane proteins. We have investigated the influence of oxygen on ^{19}F and ^{13}C NMR spectra and spin-lattice relaxation rates of a semiperfluorinated detergent, (8,8,8)-trifluoro (3,3,4,4,5,5,6,6,7,7)-difluoro octylmaltoside (TFOM) in a model membrane system, to determine the dominant paramagnetic spin-lattice relaxation and shift-perturbation mechanism. Based on the ratio of paramagnetic spin-lattice relaxation rates of ^{19}F and directly bonded ^{13}C nuclei, we conclude that the dominant relaxation mechanism must be dipolar. Furthermore, the temperature dependence of oxygen-induced chemical shift perturbations in ^{19}F NMR spectra suggests a contact interaction is the dominant shift mechanism. The respective hyperfine coupling constants for ^{19}F and ^{13}C nuclei can then be estimated from the contact shifts $\langle(\Delta\nu/\nu_0)^{^{19}\mathrm{F}}\rangle$ and $\langle(\Delta\nu/\nu_0)^{^{13}\mathrm{C}}\rangle$, allowing us to estimate the relative contribution of scalar and dipolar relaxation to ^{19}F and ^{13}C nuclei. We conclude that the contribution to spin-lattice relaxation from the oxygen induced paramagnetic scalar mechanism is negligible.

Keywords: Oxygen; Paramagnetic effects; NMR; Membranes; ^{19}F NMR; ^{13}C NMR

1. Introduction

Paramagnetic probes are commonly used in NMR studies of immersion depth and topology of membrane proteins and membrane associated amphiphiles. Such probes include doxyl spin labels which may be positioned virtually anywhere along the aliphatic chain of a lipid or fatty acid, or in the water facing headgroup [1,2]. These spin labels strongly influence nuclear spin relaxation rates and affect line broadening of signals originating near the spin labels. Consequently, differential paramagnetic effects are used to gauge relative membrane immersion depth of nuclei. Water soluble paramagnetic relaxation agents, such as free or chelated Mn^{2+} or Gd^{3+}, may also be used to determine topology, and to some extent immersion depth [3]. Alternatively, differential paramagnetic shifts obtained via species such as Eu^{3+} or Dy^{3+} in complex with the molecule under study, give topological information and can be used to refine membrane peptide or protein structure [4,5]. In an analogous manner, a paramagnetic quencher such as dioxygen, with known membrane partitioning properties, may be combined with a spin-label or fluorescent probe, anchored to a specific region of a membrane peptide or protein, to determine immersion depth via solution or solid state NMR, ESR [6] or fluorescence [7,8] spectroscopy.

* Corresponding author. Fax: +1 905 828 5425.
E-mail address: sprosser@utm.utoronto.ca (R.S. Prosser).

1090-7807/$ - see front matter © 2004 Elsevier Inc. All rights reserved.
doi:10.1016/j.jmr.2004.08.012

This paper focuses on the potential use of dioxygen[1] as a paramagnetic probe of membrane immersion depth and membrane protein topology. In particular, we report on the use of ^{19}F and ^{13}C NMR to assess the mechanism of spin-lattice relaxation enhancement and chemical shift perturbation by oxygen, using a small semiperfluorinated probe molecule, $CF_3(CF_2)_5C_2H_4$-O-maltose (TFOM) in a membrane model system. Although oxygen has been used effectively in a variety of NMR studies involving water soluble proteins [9–11], it has several unique attributes as a paramagnetic probe in NMR studies of membranes:

(1) Oxygen can be easily incorporated after equilibration at a desired partial pressure. Degassing is achieved by alternately freeze-thawing and centrifuging the sample. If gentler degassing methods are required, pressurized helium can be used to displace oxygen.
(2) Oxygen is uncharged and non-perturbing. Immersion depth, topology or local dynamics can be studied via paramagnetic effects, without the need for bulky spin-labels or fluorescent probes.
(3) In general, dipolar relaxation is governed by both a distance term, $\langle 1/r^6 \rangle$, associated with the vector between oxygen and the nuclear spin of interest, and by a spectral density term, which embodies several correlation times. These correlation times reflect intramolecular motions, oxygen exchange or diffusional rates, and electronic spin-lattice relaxation. However, the contribution to the spectral density term is dominated by electron spin-lattice relaxation, effectively reducing the analysis of paramagnetic relaxation rates to a determination of local accessibility (i.e., $\langle 1/r^6 \rangle$) [9].
(4) At modest partial pressures (20 atm, PO_2) ^1H or ^{19}F T_1s may range from 0.5 s to 50 ms, in membranes, while ^{19}F chemical shift perturbations may be as high as 5 ppm. Moreover, these paramagnetic effects are observed with minimal line broadening.
(5) Oxygen solubility ranges over an order of magnitude across a membrane or micelle [12]. Since solubility increases with local disorder of the host lipids or detergents, we observe pronounced paramagnetic gradients across membranes and micelles, permitting the measurement of immersion depth [13,14]. In studies of membrane proteins, we can further resolve protein topology since oxygen solubility is typically low in protein interiors [15].
(6) Oxygen exhibits no pronounced preference for nuclei with equivalent collisional accessibility. In contrast, lanthanide ions exhibit strong electrostatic interactions with oppositely charged groups while neutral lanthanide-chelate complexes still exhibit preferences for residues whose oxygen atoms act as coordinating nucleophiles to lanthanides [16]. Therefore, relative paramagnetic effects from oxygen are determined by depth-specific solubility and by collisional accessibility via the dipolar interaction, as discussed below.

To assess the origin of paramagnetic effects from oxygen, we describe herein measurements of spin-lattice relaxation rate enhancements of ^{19}F nuclei and directly bonded ^{13}C nuclei in TFOM, which has been inserted into a membrane. As described below, the ratio of rate enhancements, $\langle R_1^P(^{19}F)/R_1^P(^{13}C) \rangle$, confirms that the paramagnetic relaxation mechanism is dipolar (pseudo-contact) rather than contact. Results of studies of paramagnetic effects on TFOM also revealed prominent chemical shift perturbations. These perturbations are predicted to depend inversely on temperature, under the assumption of a contact shift mechanism. Details of our efforts to validate the shift mechanism are also given in this paper. We begin with a brief discussion of the model system and experiments, followed by a discussion of the theory of paramagnetic spin-lattice relaxation, as it applies to oxygen in membranes. We then present results from ^{19}F and ^{13}C NMR experiments which confirm the mechanisms for paramagnetic relaxation and shift perturbations.

2. Materials and methods

To achieve a membrane bilayer suitable for solution state NMR experiments, micelle-sized aggregates (fast tumbling bicelles), consisting of a long chain lipid (DMPC) and two mole equivalents of a detergent-like short chain lipid (DHPC) were prepared in a 100 mM pH 7.0 buffered solution of H_2O/D_2O (90/10), at a lipid weight concentration of 20% (w/w) [17,18]. For long chain- to short chain lipid molar ratios of between 0.5 and 1.0, the long-chain lipids have been shown to assemble into uniform disk-shaped bilayers, whose hydrophobic edges are capped with short chain lipids (DHPC), forming water-soluble bilayered micelles or bicelles [18]. The fast-tumbling bicelles, can be easily modified to include charged lipids, cholesterol, sphingolipids, etc. to mimic a given membrane type, while solution-state NMR spectra of amphiphiles associated with the bilayer, can be observed over a wide range of temperatures. In our experiments, (8,8,8)-trifluoro (3,3,4,4,5,5,6,6,7,7)-difluoro octylmaltoside (TFOM), obtained as a gift from C. Sanders, (Vanderbilt University) was combined with the bicelle mixtures to obtain a DMPC/TFOM ratio of 50. The resultant proton and ^{19}F NMR spectra are reasonably well resolved, while ^{19}F transverse relaxation times are sufficiently long to af-

[1] Dioxygen will be referred to simply as oxygen for the remainder of the article.

fect INEPT transfers to ^{13}C nuclei via 280 Hz 1-bond couplings. The O_2 paramagnetic relaxation rate enhancements may therefore be applied in this model system to determine precise positioning information, as shown in the following section. As discussed later in the paper, one sample was also prepared, which consisted solely of TFOM in methanol at a concentration of approximately 1 mg/ml. This sample was later pressurized to 60 atm O_2 or N_2 partial pressure, from which spectra and ^{19}F relaxation times were obtained.

Though somewhat limited by concentration (i.e., DMPC concentrations were approximately 125 mM while TFOM concentrations were approximately 2.5 mM) ^{19}F NMR spectra were easily obtained in a single scan using a standard HNC probe, with the proton channel tuned to ^{19}F at 470.3 MHz, on a Varian Inova 500 MHz spectrometer. To observe directly bonded ^{13}C nuclei from TFOM at natural abundance, a standard HSQC sequence was used in which the INEPT period was adjusted to account for a 280 Hz 1-bond CF coupling. ^{13}C spin-lattice relaxation was studied in a similar way, where $I_X C_Z$ was first converted to C_Z, which was then evolved and converted back to transverse ^{19}F magnetization (I_X) [19]. In the case of ^{13}C T_1 measurements, it was not necessary to evolve the ^{13}C chemical shifts since complete resolution of all six peaks was possible in the directly detected dimension (^{19}F). Each evolution time in the ^{13}C T_1 measurements required 9000 scans, although 1D and 2D ^{19}F NMR experiments in the presence of oxygen were performed in less time than their unoxygenated counterparts, since ^{19}F spin-lattice relaxation times were less than 100 ms at 60 atm (PO_2). To observe oxygen induced chemical shift perturbations, a 2D (^{19}F, ^{13}C) HMQC experiment was performed at either 60 atm O_2 or N_2 pressures. To optimize resolution in the indirect dimension, 512 increments were acquired, with a ^{13}C spectral width of 4500 Hz. 400 scans per increment were obtained and a repetition time of 0.15 s was used in the presence of oxygen, while one fourth as many scans and a repetition time of 0.6 s was used in the presence of nitrogen, where ^{19}F spin-lattice relaxation times are much longer. The resulting 2D spectra were referenced such that the position of the resonance associated with carbon 3 was identical. ^{19}F spin-lattice paramagnetic rates at carbon 3 are known to be smallest; therefore this referencing scheme gives an impression of the relative range of shift perturbations within TFOM.

Bicelle samples were typically pre-equilibrated under pressure for two days, before beginning NMR experiments. Sapphire NMR tubes (5 mm OD, 3 mm ID) obtained from Saphikon (Milford, NH) were used for all pressure experiments. An important consideration at oxygen partial pressures above 20 atm is the levitation effect, which occurs once the paramagnetic sample is introduced to the magnet [14]. Our solution was to implement a small polyethylene plug with a pinhole sized aperture to allow for gas exchange. The plug served to maintain the sample in the bottom of the NMR tube. We have also observed that a pressurized sample may be temporarily depressurized, quickly transferred to the magnet, then repressurized, without levitation effects; in other words, the levitation effects occur most easily when lowering the sample into position in the magnet.

3. Results and discussion

3.1. Dipolar spin-lattice relaxation enhancement by oxygen

Fig. 1 depicts the oxygen-induced ^{19}F paramagnetic rate (R_1^P) and chemical shift perturbation ($\Delta\sigma$) profile of the semiperfluorinated detergent molecule, TFOM, in a bilayer lipid environment. Note that the larger van der Waals radius of the ^{19}F atoms in comparison to ^{1}H atoms, results in a much higher fraction of *trans* conformers along the perfluorinated region of TFOM. Consequently, each difluoromethylene group in TFOM occupies a distinct average position in the host lipid bilayer, such that Angstrom resolution in immersion depth is achieved as evidenced by the steep profile of both (contact) shift perturbations and paramagnetic spin-lattice relaxation rates. In contrast, the range of ^{1}H paramagnetic spin-lattice relaxation rates is not as pronounced for lipids, due in part to the extensive dynamic averaging of oxygen environments, by most of the lipid methylene groups on the NMR time scale [20].

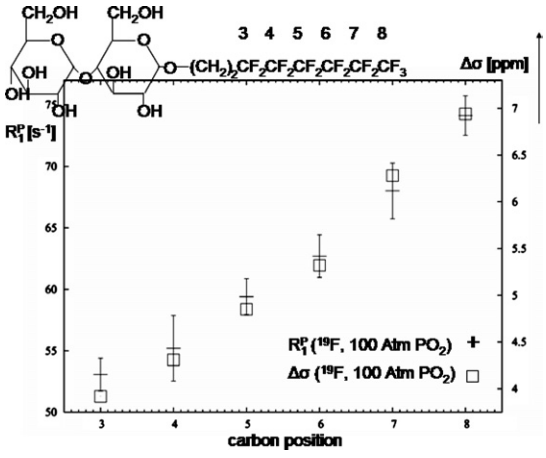

Fig. 1. Paramagnetic spin-lattice relaxation rate profile, R_1^P (crosses), and oxygen induced chemical shift perturbations, $\Delta\sigma$ (open squares), as a function of carbon position for ^{19}F nuclei in TFOM, whose structural formula is given the figure. Spectra were obtained at 500 MHz (^{1}H) field strength and an oxygen partial pressure of 100 atm PO_2.

The paramagnetic spin-lattice relaxation rate, R_1^P, is easily obtained by measuring T_1 at the desired oxygen partial pressure and at an equivalent partial pressure of nitrogen, giving

$$R_1^P = 1/T_1(\mathrm{O}_2) - 1/T_1(\mathrm{N}_2), \tag{1}$$

where such an approach also accounts for possible effects of pressure. To the extent that paramagnetic spin-lattice relaxation is acted on purely by a dipolar mechanism the rate may be described by [21,3]

$$\begin{aligned} R_1^P &= N_{\mathrm{O}_2}\tfrac{2}{15}(\mu_0/4\pi)^2\tfrac{h^2 g_e^2\mu_\beta^2\gamma_I^2\gamma_S^2}{\langle r^6\rangle}\left\{\tfrac{3\tau_1}{1+\omega_I^2\tau_1^2}+\tfrac{7\tau_2}{1+\omega_S^2\tau_2^2}\right\},\\ 1/\tau_1 &= 1/\tau_D + 1/T_{1e},\\ 1/\tau_2 &= 1/\tau_D + 1/T_{2e}. \end{aligned} \tag{2}$$

N_{O_2} refers to the (immersion depth-specific) probability distribution of oxygen in the membrane, while γ_I and γ_S designate the nuclear and electron gyromagnetic ratios. The critical variables in the above expression for R_1^P include the depth dependent N_{O_2}, the motionally averaged oxygen—nuclear spin distance term, $\langle 1/r^6\rangle$, and the oxygen diffusional correlation time, τ_D. The electronic relaxation time of oxygen, which is estimated to be 7.5 ps, [22] is significantly less than relaxation times observed for common relaxation agents such as Gd^{3+}, Mn^{2+}, or doxyl spin-labels. The correlation time, τ_D, associated with oxygen diffusion, is approximated by [23]

$$\tau_D = d^2/2D, \tag{3}$$

where d represents the effective collision diameter and D represents the diffusion constant. Using a collision diameter of 0.36 nm and a diffusion rate of $2\times10^{-9}\ \mathrm{m^2\ s^{-1}}$, we obtain a correlation time of 32 ps in water, although this value can be significantly lower in membranes [12]. Using the above values for τ_D and T_{1e}, we obtain $\tau_1 \approx 5.8$ ps in water while approximations of O_2 diffusion rates in membranes [12] allow us to estimate $\tau_1 \approx 3.6$ ps in the bilayer interior. Thus, at a fluorine Larmor frequency of 470.3 MHz, $(\omega_0\tau_D)^2 \ll 1$ and $(\omega_0\tau_1)^2 \ll 1$. In this extreme narrowing limit, the rate expression simplifies to the following

$$R_1^P = N_{\mathrm{O}_2}\frac{2}{15}(\mu_0/4\pi)^2\frac{h^2 g_e^2\mu_\beta^2\gamma_I^2\gamma_S^2}{\langle r^6\rangle}\{3\tau_1+7\tau_2\}. \tag{4}$$

The above spectral density term in parenthesis is dominated by the electronic relaxation correlation time and is relatively constant at a given field strength. Therefore, the observed rate will depend only on the local topology or structure term, $1/\langle r^6\rangle$, and on the immersion depth-dependent solubility term, N_{O_2}. Finally, in any detailed analysis of paramagnetic relaxation rates of flexible or highly dynamic conformers, we must consider that the ensemble distribution of conformations, and immersion depths associated with each label.

To confirm that the dipolar interaction is the dominant source of paramagnetic spin-lattice relaxation, we consider the effect of relaxation on the ^{19}F nuclei and their directly bonded ^{13}C counterparts. In particular, we may write the ratio of paramagnetic spin-lattice relaxation rates for a given CF pair (at a given immersion depth) as

$$\frac{R_1^P(^{19}\mathrm{F})}{R_1^P(^{13}\mathrm{C})} = \frac{\gamma_{^{19}\mathrm{F}}^2}{\gamma_{^{13}\mathrm{C}}^2}\frac{\langle r^6_{^{13}\mathrm{C}-\mathrm{O}_2}\rangle}{\langle r^6_{^{19}\mathrm{F}-\mathrm{O}_2}\rangle}, \tag{5}$$

where we assume that the depth specific oxygen probability distribution, N_{O_2}, and diffusional correlation time, τ_D, will be common to each CF pair, and thus factor out in the above ratio. In contrast, the accessibility as measured by $\langle 1/r^6\rangle$ will be greater for the fluorine nuclei which serve to shield the carbon nuclei from oxygen. Using the CPK structure of TFOM, we can numerically estimate the ratio of accessibilities, $\langle r^6_{^{13}\mathrm{C}-\mathrm{O}_2}\rangle/\langle r^6_{^{19}\mathrm{F}-\mathrm{O}_2}\rangle$. The simplest way to calculate $\langle 1/r^6\rangle$ is to first surround the nucleus of interest in a sphere, whose radius is reasonably beyond the extent of influence of a paramagnetic species (i.e., 10 Å). A Cartesian grid system is then established within the sphere with a grid point spacing of 0.10 Å in each dimension [10]. At each grid point, we must first determine if any atom of TFOM overlaps with the grid point, within the van der Waals radius. Second, we must determine if the grid point is too close to the nucleus of interest—i.e., the point of closest approach should be the sum of the van der Waals radius of the nucleus of interest (either ^{19}F or ^{13}C) and the radius of oxygen. A simple weighted average of $1/r^6$ is then considered for allowable grid points. In studies of water soluble proteins the weighting factor (N_{O_2}) is a constant (all points outside the molecule are equally probable for occupation by oxygen). However, in membranes the weighting factor depends explicitly on immersion depth [13]. The resultant average $\langle r^6_{^{13}\mathrm{C}-\mathrm{O}_2}\rangle/\langle r^6_{^{19}\mathrm{F}-\mathrm{O}_2}\rangle$ was computed to be 2.34 giving the following theoretical value for the ratio of paramagnetic rates,

$$\frac{R_1^P(^{19}\mathrm{F})}{R_1^P(^{13}\mathrm{C})} = \frac{\gamma_{^{19}\mathrm{F}}^2}{\gamma_{^{13}\mathrm{C}}^2}\frac{\langle r^6_{^{13}\mathrm{C}-\mathrm{O}_2}\rangle}{\langle r^6_{^{19}\mathrm{F}-\mathrm{O}_2}\rangle} = 14.3\times 2.34 = 33. \tag{6}$$

^{19}F paramagnetic rates can be routinely measured with an uncertainty of a few percent. However, it is difficult to obtain reliable estimates of R_1^P for ^{13}C nuclei both because these rates are considerably smaller and because the natural abundance ^{13}C signal is significantly weaker than that from ^{19}F. Fig. 2 shows a typical series of ^{13}C-edited ^{19}F spectra of TFOM in a bicelle mixture, under the influence of oxygen at 60 atm, PO_2. In this series, the peak intensities are proportional to ^{13}C Zeeman magnetization, C_Z, which is indirectly evolved in the usual way. Table 1 summarizes the results of the ^{19}F T_1 measurements and indirect measurements of ^{13}C T_1 both under nitrogen pressure and equivalent pressures of

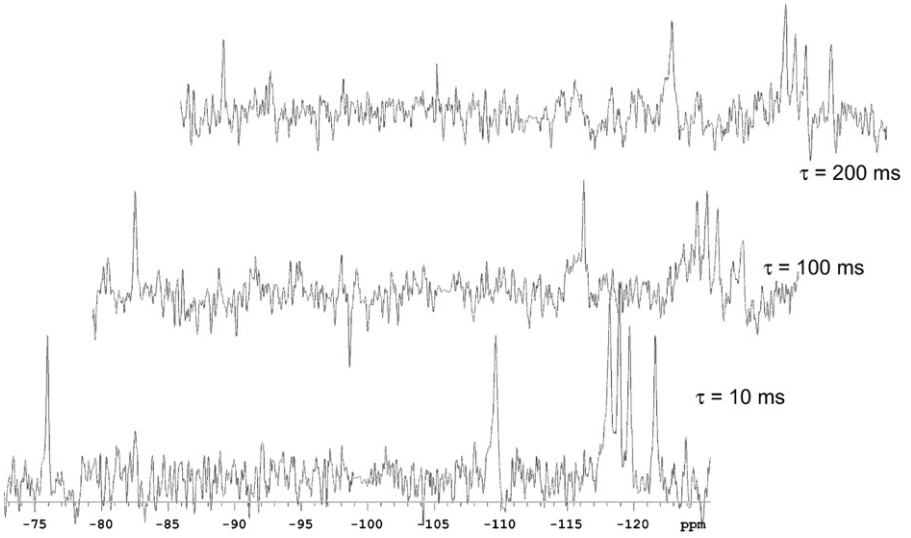

Fig. 2. Representative ^{19}F NMR spectra of TFOM, in which directly bonded ^{13}C Zeeman magnetization, C_Z, is indirectly evolved for τ ms. Each spectrum required 9000 scans and the complete series of 9 τ values was obtained in 15 h. The O_2 partial pressure was 60 atm and the temperature was maintained at 25 °C.

Table 1
^{19}F and ^{13}C O_2-induced paramagnetic effects vs chain position

TFOM position	3	4	5	6	7	8
^{13}C T_1 (s)	0.53 ± 0.17	0.38 ± 0.1	0.74 ± 0.2	0.38 ± 0.1	0.49 ± 0.1	0.66 ± 0.18
$+O_2$:^{13}C T_1 (s)	0.25 ± 0.06	0.26 ± 0.18	0.45 ± 0.19	0.27 ± 0.09	0.16 ± 0.06	0.18 ± 0.06
$+O_2$:^{13}C R_1^P (s^{-1})	2.2	1.3	0.9	1.1	4.3	3.9
$+O_2$:^{19}F R_1^P (s^{-1})	37.7 ± 0.2	38.7 ± 0.1	40.6 ± 0.2	42.2 ± 0.2	46.6 ± 0.1	53.3 ± 0.1
$+O_2$:$\Delta\sigma$ (^{13}C)		−0.01	0.01	0.03	0.04	0.09
$+O_2$:$\Delta\sigma$ (^{19}F)		0.70	1.23	1.74	2.81	3.47

Indirectly detected ^{13}C spin lattice relaxation rates are shown at 60 atm nitrogen and oxygen partial pressures, respectively. The corresponding paramagnetic ^{13}C spin-lattice relaxation rates are shown below, along with ^{19}F paramagnetic spin-lattice relaxation rates, for comparison. The experimentally determined average of $R_1^P(^{19}\mathrm{F})/R_1^P(^{13}\mathrm{C})$ is determined to be 26 ± 8. The last 2 rows in the table, compare ^{19}F and ^{13}C chemical shift perturbations due to oxygen. Without an internal standard (which would also shift from oxygen), we referenced the chemical shift difference, on going from 60 atm N_2 to 60 atm O_2, to 0 ppm for both ^{19}F and ^{13}C at position 3.

oxygen. As shown in the table, the experimentally determined ratio of paramagnetic spin-lattice relaxation rates is estimated to be $\langle R_1^P(^{19}\mathrm{F})/R_1^P(^{13}\mathrm{C})\rangle = 26 \pm 8$, averaged over all six carbon positions, which agrees within uncertainty limits, with the above theoretically predicted value. However, we must also consider the potential contribution of other paramagnetic relaxation mechanisms to either ^{19}F or ^{13}C.

3.2. Other potential sources of spin-lattice relaxation enhancement

The well known Solomon–Bloembergen equations proposed that paramagnetic spin-lattice relaxation may originate from both a dipolar mechanism, as described above, and from a scalar or contact mechanism given as [21]

$$R_1^P = \frac{2}{3}\left(\frac{A_n}{\hbar}\right)^2 S(S+1)\left\{\frac{\tau}{(1+\omega_e^2\tau^2)}\right\}, \tag{7}$$

where

$$\tau^{-1} = \tau_D^{-1} + 1/T_{1e}. \tag{8}$$

A_n is the isotropic (hyperfine) electron-nuclear spin coupling constant, while ω_e represents the electron Larmor frequency. Note that a "$\langle 1/r^6\rangle$" distance term is blatantly absent in this expression, reinforcing the notion that the contact interaction results from unpaired electron spin density at the nucleus of interest. As such, the magnitude of the contact interaction will depend on collisional accessibility, in a manner similar to the way in which ESR spin labels are quenched by dioxygen. Since the hyperfine coupling constant is explicitly involved in the contact shift, it is possible to estimate the respective constants, A_{19_F} and A_{13_C}, by measuring oxygen induced chemical shift perturbations for ^{19}F nuclei and the directly bonded ^{13}C nuclei, as discussed below. Thus, in the next section, once we have determined the hyperfine coupling constants, we will make use of

the above expression, and revisit the issue of the relative contribution of a contact mechanism on observed paramagnetic rates for ^{13}C and ^{19}F nuclei, in the presence of oxygen.

3.3. Sources of chemical shift perturbation

In this study, we observed oxygen-induced shift perturbations, as high as 3.5 ppm in the ^{19}F dimension and 0.1 ppm in the ^{13}C dimension. A 2D (^{19}F, ^{13}C) HMQC spectrum was obtained at 60 atm O_2 and 60 atm N_2 to determine oxygen induced ^{19}F and ^{13}C shifts, which are reported in Table 1. In this section we consider three possible sources for the origin of oxygen-induced chemical shift perturbations observed on ^{13}C and ^{19}F nuclei: the pseudocontact (dipolar) mechanism, a magnetic susceptibility variation, and a contact (scalar) mechanism.In solution NMR experiments, dipolar paramagnetic mechanisms may also give rise to a dipolar or pseudocontact shift, expressed in terms of the magnetic susceptibility tensor, χ, as [3]

$$\left(\frac{\Delta\nu}{\nu_0}\right)^{\mathrm{dip}} = \frac{1}{4\pi 2r^3}\left[(3\cos^2\theta - 1)\left(\frac{2}{3}\chi_{ZZ} - \frac{1}{3}\chi_{XX} - \frac{1}{3}\chi_{YY}\right) + \sin^2\theta\cos 2\Omega \times (\chi_{XX} - \chi_{YY})\right], \quad (9)$$

where r represents the electron-nuclear vector, whose orientation in the molecular coordinate system is defined by the polar angles (θ, Ω). Clearly, if the paramagnetic species is not specifically coordinated with the molecule under study, the dipolar contribution will average to zero. Thus, we discount the dipolar mechanism as a source of oxygen induced chemical shift perturbations for either ^{13}C or ^{19}F.

A second mechanism to consider as a source of chemical shift perturbations is that due to local magnetic susceptibility variations, arising from non-homogeneous oxygen solubility. However, if a susceptibility variation was the dominant paramagnetic shift mechanism, proton shifts $(\Delta\nu/\nu_0)$ would be expected to be comparable to those of ^{19}F since the paramagnetic shifts would be in proportion to the gyromagnetic ratio. Since there are no detectable proton chemical shift perturbations arising from oxygen in the host lipids, we conclude that susceptibility variations do not contribute to shift perturbations.

Non-coordinating paramagnetic species, such as oxygen, may affect a chemical shift perturbation through a contact mechanism, where the resultant shift is expressed as [3]

$$\left(\frac{\Delta\nu}{\nu_0}\right)^{\mathrm{con}} = \frac{A_n}{\hbar}\frac{g_e\mu_B S(S+1)}{3\gamma_n kT}. \quad (10)$$

To definitively confirm the contact mechanism as the source of chemical shift perturbations, it would seem sensible to monitor the temperature dependence of the oxygen induced shifts [24]. Unfortunately, this dependence is difficult to measure since membrane order parameter gradients are sensitive to temperature and oxygen solubility depends on local order. In fact, paramagnetic shifts (and paramagnetic relaxation rates) tend to decrease with temperature, due presumably to reduced oxygen solubility from membrane ordering. Furthermore, a significant waiting period (>12 h) is necessary to allow oxygen to adopt its equilibrium distribution at each temperature. To minimize the effect of changes in the oxygen solubility through membrane ordering, we considered the temperature dependence of ^{19}F shifts of TFOM in methanol. At concentrations below the critical micelle concentration of TFOM we expect the temperature dependent ordering properties and consequent oxygen solubilities to be consistent with a typical liquid. Moreover, to account for the temperature dependence of oxygen solubility we can normalize the oxygen dependent shifts ($\Delta\sigma$) by dividing by the corresponding ^{19}F paramagnetic spin-lattice relaxation rates, which are roughly proportional to concentration. The resultant scaled chemical shift profiles, shown in Fig. 3, are nearly consistent with the predicted inverse temperature dependence, with the exception of position 3, which we believe undergoes a conformational change with temperature. Successive difluoromethylenes are well known to favor an *all trans* conformation, due to steric hindrance. However, the difluoromethylene at position 3 is adjacent to a (protonated) methylene group and would thus be free to adopt a higher fraction of gauche conformers. This property is certainly expected to be sensitive to temperature. Thus, we interpret the overall normalized shift data to be consistent with a contact shift mechanism.

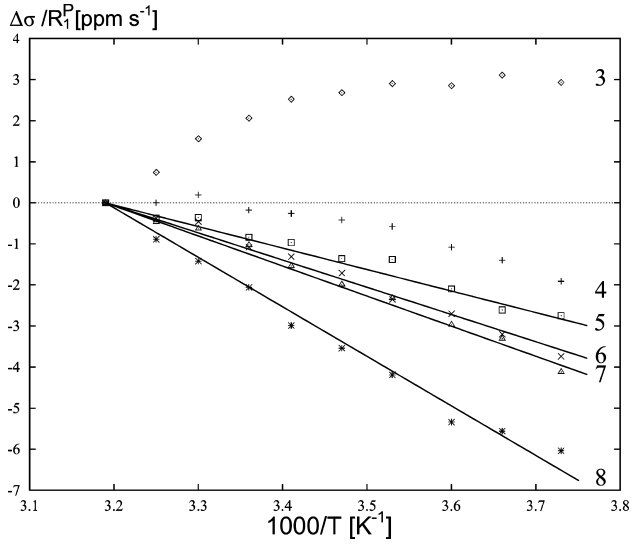

Fig. 3. T_1-scaled ^{19}F chemical shift perturbations, $\Delta\sigma/R_1^P$, of TFOM in methanol as a function of inverse temperature. Shifts of labeled positions 3–8 are referenced to their absolute values at 40 °C.

3.4. Spin-lattice relaxation: the scalar mechanism revisited

Assuming that the shift is entirely of a contact origin, we can next turn our attention toward the determination of the hyperfine coupling constants, A_n, for both ^{19}F and ^{13}C nuclei. Solving for the coupling constant we obtain

$$\frac{A_n}{\hbar} = \left(\frac{\Delta\nu}{\nu_0}\right)^{\text{con}} \frac{3\gamma_n kT}{g_e\mu_B S(S+1)}. \tag{11}$$

Since the contact shifts reported in Table 1, were determined relative to position 3 we might envisage that in the presence of an absolute chemical shift reference that a sensible upper limit to the ^{19}F and ^{13}C chemical shifts is on the order of 0.2 and 7.0 ppm.[2] Using reported values for g_e and μ_B [3], we thus obtain $(A_{^{19}\text{F}}/\hbar) \leqslant 6.1 \times 10^5$ rad s^{-1} and $(A_{^{13}\text{C}}/\hbar) \leqslant 4.7 \times 10^3$ rad s^{-1} at 40 °C. Using Eq. (10), and estimating an effective correlation time, τ, of 5 ps, we obtain $R_1^P(^{19}\text{F}) = 0.026$ Hz and $R_1^P(^{13}\text{C}) = 1.5 \times 10^{-6}$ Hz as estimates for the spin-lattice relaxation rate arising purely from the scalar interaction. Thus, we conclude that the contribution to oxygen induced paramagnetic spin-lattice relaxation arising from the scalar mechanism is negligible for either ^{19}F or ^{13}C nuclei.

4. Conclusions

In this paper, we have examined the possible origin of dioxygen induced paramagnetic relaxation, using solution NMR. By considering a ratio of the paramagnetic rates of the ^{19}F nuclei to those of the directly bonded ^{13}C nuclei, $R_1^P(^{19}\text{F})/R_1^P(^{13}\text{C})$, in membrane bound TFOM, we determined that within experimental error, the pseudocontact or dipolar mechanism is the dominant source of paramagnetic relaxation under oxygen partial pressures of 20 atm or more. Conversely, the oxygen induced chemical shift perturbations were determined to originate from a contact (scalar) mechanism, based on a temperature dependence of ^{19}F chemical shift perturbations of TFOM in methanol. Small contact shifts were also observed to the directly bonded ^{13}C nuclei. An analysis of oxygen-induced ^{19}F and ^{13}C chemical shift perturbations of TFOM in a membrane, provided a means of estimating the ^{19}F and ^{13}C hyperfine coupling constants. These coupling constants could then be used to assess the feasibility of scalar spin-lattice relaxation. The predicted paramagnetic spin-lattice relaxation rates arising from the scalar mechanism were determined to be negligible both for the case of ^{19}F and ^{13}C nuclei.

[2] This upper bound estimate is based on our knowledge of the overall oxygen solubility profile [14].

Assuming that paramagnetic spin-lattice relaxation arises solely from a dipolar interaction, we may conclude that similar paramagnetic effects should be observed on high gamma nuclei, such as ^{1}H. By now, several key solution NMR articles have appeared in which paramagnetic ^{1}H spin-lattice relaxation effects from oxygen, are used to evaluate protein topology [10], dynamics, and oxygen diffusion and binding pathways in heme proteins [25]. These papers demonstrate that paramagnetic spin-lattice relaxation rates from oxygen can be used to quantitatively assess structure and folds of proteins. In this paper, we make the additional observation of ^{13}C contact shifts which clearly correlate with membrane immersion depth. Although the effects are small, we have observed significantly larger ^{13}C shift perturbations in CH_2 and CH_3 systems, implying the possibility for assessing topology from ^{13}C contact shifts in solution NMR studies of membrane peptides and membrane proteins. The measurement of R_1^P for high gamma nuclei (^{19}F or ^{1}H) and accompanying measurements of ^{13}C contact shifts, may prove to be useful in membrane protein studies since each measurement probes topology differently; R_1^P depends on both $\langle 1/r^6\rangle$ and a correlation time associated with local oxygen diffusion, τ_D, while $(\Delta\nu/\nu_0)^{^{13}\text{C}}$ depends only on the local O_2 collisonal accessibility.

Note added in proof

The Solomon–Bloembergen (SBB) equations do not adequately describe a freely diffusing paramagnet, particularly where the electronic spin–lattice relaxation time is short. In particular, analytical descriptions of dipolar relaxation by Hwang and Freed (J. Chem. Phys. 63 (1975) 4017) and Ayant et al (J. Phys. 36 (1975) 991) invoke a b^3 term, where b represents the distance of closest approach of the paramagnet to the nuclear spin. Our cruder version, used in this paper, made use of a volume integral of $1/r^6$, which approximates $1/b^3$ for small molecules, though we must also account for the concentration gradient of oxygen in the membrane. Furthermore, the spectral density terms in the Freed and Ayant formalisms are significantly different from those in the SBB. However, in our case, we treat ratios of paramagnetic relaxation rates for CF pairs, in which case the spectral density terms factor out for short T_{1e}.

Acknowledgments

RSP gratefully acknowledges the American Chemical Society (PRF AC Grant 376620) and the Natural Sciences and Engineering Research Council of Canada (NSERC), for generous funding support. The authors

are also grateful to R.G. Bryant for many stimulating discussions.

References

[1] L.R. Brown, C. Bosch, K. Wüthrich, Location and orientation relative to the micelle surface for glucagon in mixed micelles with dodecylphosphocholine—EPR and NMR studies, Biochim. Biophys. Acta 642 (1981) 296–312.
[2] P. Damberg, J. Jarvet, A. Graslund, Micellar systems as solvents in peptide and protein structure determination, Methods Enzymol. 339 (2001) 271–285.
[3] I. Bertini and C. Luchinat, NMR of Paramagnetic Molecules in Biological Systems, Benjamin/Cummings, Menlo Park, 1986.
[4] I. Bertini, C. Luchinat, A. Rosato, The solution structure of paramagnetic metalloproteins, Prog. Biophys. Mol. Biol. 66 (1996) 43–80.
[5] L. Banci, I. Bertini, C. Luchinat, 2-Dimensional nuclear magnetic resonance spectra of paramagnetic systems, Methods Enzymol. 239 (1994) 485–514.
[6] C. Altenbach, T. Marti, H.G. Khorana, W.L. Hubbell, Transmembrane protein structure—spin labeling of bacteriorhodopsin mutants, Science 248 (1990) 1088–1092.
[7] J. Kim, M.G. McNamee, Topological disposition of Cys 222 in the alpha-subunit of nicotinic acetylcholine receptor analyzed by fluorescence-quenching and electron paramagnetic resonance measurements, Biochemistry 37 (1998) 4680–4686.
[8] V. Narayanaswami, J.G. Kim, M.G. McNamee, Protein–lipid interactions and torpedo Californica nicotinic acetylcholine receptor function. 1. Spatial disposition of cysteine residues in the gamma-subunit analyzed by fluorescence-quenching and energy-transfer measurements, Biochemistry 32 (1993) 12413–12419.
[9] C.L. Teng, R.G. Bryant, Experimental measurement of nonuniform dioxygen accessibility to ribonuclease A surface and interior, J. Am. Chem. Soc. 122 (2000) 2667–2668.
[10] G. Hernandez, C.L. Teng, R.G. Bryant, D.M. LeMaster, O2 penetration and proton burial depth in proteins: applicability to fold family recognition, J. Am. Chem. Soc. 124 (2002) 4463–4472.
[11] T.S. Ulmer, I.D. Campbell, J. Boyd, The effects of dissolved oxygen upon amide proton relaxation and chemical shift in a perdeuterated protein, J. Magn. Reson. 157 (2002) 181–189.
[12] S.J. Marrink, H.J.C. Berendsen, Permeation process of small molecules across lipid membranes studied by molecular dynamics simulations, J. Phys. Chem. 100 (1996) 16729–16738.
[13] R.S. Prosser, P.A. Luchette, P.W. Westerman, Using O2 to probe membrane immersion depth by F-19 NMR, Proc. Natl. Acad. Sci. USA 97 (2000) 9967–9971.
[14] R.S. Prosser, P.A. Luchette, P.W. Westerman, A. Rozek, R.E.W. Hancock, Determination of membrane immersion depth with O2: a high-pressure F-19 NMR study, Biophys. J. 80 (2001) 1406–1416.
[15] P.A. Luchette, R.S. Prosser, C.R. Sanders, Oxygen as a paramagnetic probe of membrane protein structure by cysteine mutagenesis and F-19 NMR spectroscopy, J. Am. Chem. Soc. 124 (2002) 1778–1781.
[16] A.M. Petros, L. Mueller, K.D. Kopple, NMR identification of protein surfaces using paramagnetic probes, Biochemistry 29 (1990) 10041–10048.
[17] R.R. Vold, R.S. Prosser, A.J. Deese, Isotropic solutions of phospholipid bicelles: a new membrane mimetic for high-resolution NMR studies of polypeptides, J. Biomol. NMR 9 (1997) 329–335.
[18] P.A. Luchette, T.N. Vetman, R.S. Prosser, R.E.W. Hancock, M.P. Nieh, C.J. Glinka, S. Kreuger, J. Katsaras, Morphology of fast-tumbling bicelles: a small angle neutron scattering and NMR study, Biochim. Biophys. Acta 1513 (2001) 83–94.
[19] N.A. Farrow, O.W. Zhang, J.D. Forman-Kay, L.E. Kay, A heteronuclear correlation experiment for simultaneous determination of N-15 longitudinal decay and chemical-exchange rates of systems in slow equilibrium, J. Biomol. NMR 4 (1994) 727–734.
[20] S.A. Wahid, I. Batruch, and R.S. Prosser (unpublished results).
[21] I. Solomon, N. Bloembergen, Nuclear magnetic interactions in the HF molecule, J. Chem. Phys. 25 (1956) 261–266.
[22] C.L. Teng, H. Hong, S. Kiihne, R.G. Bryant, J. Magn. Reson. 148 (2001) 31–34.
[23] A. Abragam, Principles of Nuclear Magnetism, Clarendon Press, Oxford, 1961.
[24] G.N. La Mar, G.R. Eaton, R.H. Holm, F.A. Walker, Proton magnetic resonance investigation of antiferromagnetic oxo-bridged ferric dimers and related high-spin monomeric ferric complexes, J. Am. Chem. Soc. 95 (1973) 63–75.
[25] L. McNaughton, G. Hernandez, D.M. LeMaster, Equilibrium O2 distribution in the Zn2+-protoporphyrin IX deoxymyoglobin mimic: application to oxygen migration pathway analysis, J. Am. Chem. Soc. 125 (2003) 3813–3820.